Journal of Materials Chemistry B

PAPER

View Article Online
View Journal | View Issue

Cite this: J. Mater. Chem. B, 2018, 6, 6842

Light-driven self-powered biosensor for ultrasensitive organophosphate pesticide detection *via* integration of the conjugated polymer-sensitized CdS and enzyme inhibition strategy†

Panpan Gai, Shuxia Zhang, Wen Yu, Haiyin Li and Feng Li *

Received 30th August 2018,
Accepted 27th September 2018

DOI: 10.1039/c8tb02286k

rsc.li/materials-b

Herein, a light-driven self-powered biosensor based on a photoelectrochemical enzymatic fuel cell (PEFC) was proposed for ultrasensitive organophosphate pesticide (OP) detection. To construct this fuel cell, poly(3,4-ethylenedioxythiophene)-sensitized CdS quantum dot (PEDOT/CdS) photoanode and multiwalled carbon nanotubes/gold nanoparticals/bilirubin oxidase (CNTs/AuNPs/BOD) biocathode were elaborately designed. Initially, the enzyme acetylcholinesterase (AChE) immobilized on the CdS/PEDOT photoanode could hydrolyze acetylthiocholine iodide (ATCh) into thiocholine as the electron donor to enhance the charge separation efficiency; thus, PEFC produced relatively high open circuit voltage (E^{OCV}) upon illumination. OPs could inhibit the AChE enzymatic catalytic activity on hydrolysis, and in this case, a smaller E^{OCV} obtained. Thus, based on the constructed PEFC, self-powered biosensing of OPs was realized, and the detection limit was as low as 0.012 ng mL^{-1} (S/N = 3), which was comparable or superior to those of the reported methods. In this study, we not only constructed a facile, ultrasensitive and low-cost sensing platform for OP detection, but also provided an ingenious idea for designing light-driven self-powered biosensing based on PEFC.

1. Introduction

Self-powered biosensors have attracted considerable attention due to their many advantages: no need of an external power source, simple instrumentation, miniaturization and low cost;[1–5] they have exhibited promising potential in human disease diagnosis,[6–9] food safety[3,10] and environmental monitoring.[10–15] In fact, most self-powered biosensors are based on enzymatic fuel cells (EFC), in which the fundamental signal is the performance output of EFC.[16–18] However, it is still operated at the expense of enzyme and fuel consumption. In addition, the bioelectrocatalysis mechanism of the anodic enzymes, such as glucose oxidase, is an inherently debatable issue for glucose oxidation.[19,20] Recently, combining the photoelectrode with the enzyme electrode to construct a photoelectrochemical biofuel cell has aroused great interest because solar energy can be considered as a cleaner and better alternative power source.[21,22] For example, a TiO_2 nanotube photoanode has been constructed to achieve direct oxidization of fuel glucose or cofactor NADH upon illumination.[23,24] Nevertheless, there are few publications on light-driven self-powered biosensors. For example, Chen's group constructed a self-powered cathodic photoelectrochemical biosensor based on hybrid PbS quantum dots/nanoporous NiO film nanostructures for glucose bioanalysis.[25] In addition, a self-powered cathodic photoelectrochemical aptasensor was reported based on Au nanoparticle-decorated g-C_3N_4 nanosheets for the detection of oxytetracycline.[26] However, they all focused on the cathodic photoelectrochemical biosensing design. Up to now, various semiconductor materials with different optical absorptions are available for the solar cell.[27,28] Moreover, the co-sensitized structures formed by the p–n heterojunction between two semiconductor materials with suitable band gaps can efficiently separate electron–hole pairs and further effectively promote the photoelectric properties of the photocatalyst. Inspired by this, we intend to develop an efficient light-driven self-powered biosensor based on co-sensitized structure photoanode, which not only significantly enhances the utilization of visible light, but also effectively promotes charge separation, thus favoring the increase in photocurrent.

College of Chemistry and Pharmaceutical Sciences, Qingdao Agricultural University, Qingdao 266109, P. R. China. E-mail: lifeng@qau.edu.cn

† Electronic supplementary information (ESI) available: The illustration of the procedure of ITO/PDDA/CdS/PEDOT/AChE preparation and the photoelectrochemical mechanism for OPs determination; TEM image of PEDOT; CVs of the CNTs/AuNPs modified CP in PB saturated with N_2 or O_2; comparison of the as-prepared self-powered sensor for detection of pesticides with other AChE-based biosensors. See DOI: 10.1039/c8tb02286k

Organophosphate pesticides (OPs) play an important role in insect control, but the human and animal toxicities of OPs make them a societal health and environmental concern.[29] Although various biosensors have been developed such as organophosphorus hydrolase-based biosensors,[30] enzyme-inhibition-based biosensors,[31–33] immunosensors,[34] photoelectrochemical biosensors,[35,36] and colorimetric sensors,[37] the methods used for preparing these biosensors are time consuming and/or require high cost, sophisticated instrumentation and highly trained technicians, which limit their applications in rapid analysis. Thus, it is urgently needed to develop simple, rapid, accurate and ultrasensitive assays for monitoring OPs.

Herein, we reported a light-driven self-powered biosensor based on a photoelectrochemical enzymatic fuel cell (PEFC) for ultrasensitive OP (chlorpyrifos as the model) detection *via* integration of the conjugated polymer-sensitized CdS and enzyme inhibition strategy. As shown in Scheme 1, the constructed PEFC comprised a conjugated polymer poly(3,4-ethylenedioxythiophene) (PEDOT)-sensitized CdS quantum dot (PEDOT/CdS) photoanode and CNTs/AuNPs/BOD biocathode upon illumination. For the photoanode, the employed PEDOT/CdS acted as the light-harvesting material to form a bi-layer heterojunction structure, which was in favor of the separation efficiency of hole–electron pairs in the absence of target OPs; the immobilized acetylcholinesterase (AChE) could hydrolyze acetylthiocholine iodide (ATCh) to thiocholine. Upon light irradiation, the electron donor thiocholine could consume the holes to enhance the efficiency of charge separation. Meanwhile, the separated electrons could transfer to the biocathode and react with oxygen by biocatalysis of the CNTs/AuNPs/BOD biocathode, thus producing high open circuit voltage (E^{OCV}) of PEFC. In the presence of OPs, they could be selectively recognized by the enzyme AChE, which significantly inhibited its catalytic activity of the hydrolysis reaction. As a result, the reduced thiocholine could lower the separation efficiency of hole–electron pairs, resulting in decrease in E^{OCV}. Consequently, the light-driven self-powered biosensor for ultrasensitive OP detection was realized according to E^{OCV} variation. In this study, we not only proposed a highly sensitive, low-cost, simple, and real-time method for OP assay but also provided an ingenious idea for designing a light-driven self-powered biosensing platform.

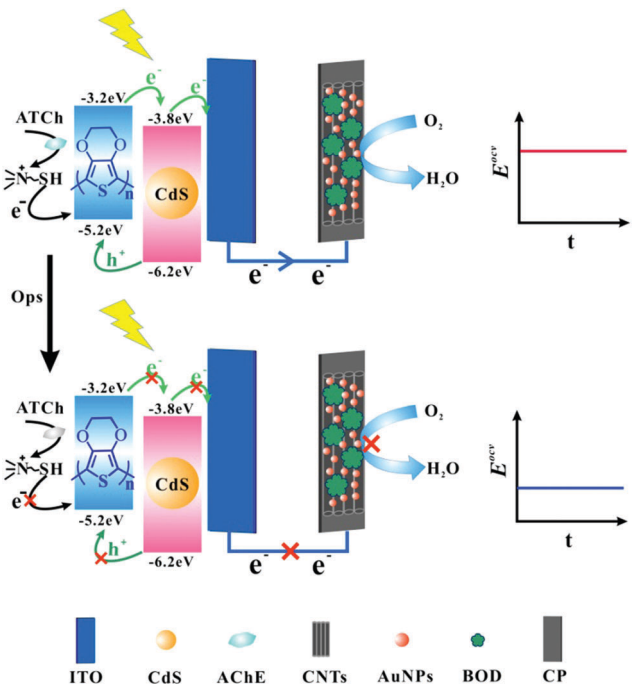

Scheme 1 Schematic illustration of the principle of PEFC-based self-powered biosensing strategy for OP assay.

2. Experimental

2.1 Materials and reagents

Acetylcholinesterase (AChE), acetylthiocholine iodide (ATCh) and chlorpyrifos were obtained from Aladdin Industrial Corporation (Shanghai, China). CdS QDs were purchased from Najingtech (Hangzhou, China). 3,4-Ethoxylenedioxythiophene (EDOT), NaCl, NaH_2PO_4 and Na_2HPO_4 were purchased from Energy Chemical (Shanghai, China). Bilirubin oxidase (BOD, E.C. 1.3.3.5, from *Myrothecium verrucaria*) and poly(diallyldimethylammonium chloride) (PDDA, 20% in water (w/w), M_w = 200 000–350 000) were purchased from Sigma-Aldrich (St. Louis, MO, USA). Carbon nanotubes (CNTs) were purchased from JCNANO (Shanghai, China). Chloroauric acid ($HAuCl_4{\cdot}4H_2O$) was obtained from Shanghai Chemical Reagent Co. Ltd (Shanghai, China). AuNPs were prepared according to a previously reported method by adding sodium citrate solution to boiling $HAuCl_4$ solution.[38] The reagents were of analytical grade and used without further purification or treatment. Ultrapure water (resistivity >18.2 MΩ cm at 25 °C) obtained from a Milli-Q water purification system (Millipore Corp., Bedford, MA, USA) was used throughout the experiments. Phosphate buffer (PB, 0.1 M, pH 7.4) was used as the supporting electrolyte.

2.2 Apparatus and instrumentation

Transmission electron microscopy (TEM) images were recorded on a HT7700 microscope (Hitachi, Japan) operated at 100 kV. The PEC measurements were performed with a Zahner PEC measurement system (Zahner, Germany). Photocurrent experiments were carried out at room temperature using a conventional three-electrode system; the bare or modified ITO electrode with an area of 1 cm^2 (1 × 1 cm) was used as the working electrode, and an Ag/AgCl electrode and a platinum wire were employed as the reference electrode and counter electrode, respectively. Electrochemical impedance spectroscopy (EIS) was performed on an Autolab electrochemical workstation (Metrohm, Netherland) at an alternating current voltage of 5 mV amplitude over a frequency range of 0.01–100 kHz in KCl solution (0.1 M) containing $[K_3Fe(CN)_6]/[K_4Fe(CN)_6]$ (5.0 mM, 1 : 1) mixture as the redox probe. Cyclic voltammetry measurements were performed on an Autolab electrochemical workstation (Metrohm, Netherland) using a three-electrode system: the fabricated biocathode as the working electrode, a Pt wire as the counter electrode, and an Ag/AgCl electrode as the reference electrode. The open circuit voltage (E^{OCV}) of PEFC

was measured by connecting the photoanode and the biocathode placed in the electrolytic cell, and the procedure was performed on the Zahner PEC measurement system (Zahner, Germany).

2.3 Fabrication of the photoanode

First, 100 μL of 1% PDDA solution was dropped on a bare ITO electrode surface for 0.5 h at room temperature to form an ITO/PDDA electrode, which was rinsed with ultrapure water. Then, 50 μL of 2 μM CdS QDs was dropped on the electrode surface and dried at ambient temperature to obtain the ITO/PDDA/CdS electrode, and the prepared electrode was rinsed with 0.1 M PB (pH 7.4). Subsequently, a PEDOT film *via* EDOT electropolymerization was deposited on the above electrode by referring to a previous report with a few modifications. In detail, the ITO/PDDA/CdS electrode was immersed in 5 mL PB solution containing 54 μL EDOT. Then, the electropolymerization of EDOT was performed at a constant potential of +1.0 V for 800 s to obtain the PEDOT film on the electrode surface. Finally, the obtained ITO/PDDA/CdS/PEDOT electrode was coated with 20 μL AChE solution (10 U mL^{-1}) and incubated at 25 °C for 1 h; then, it was washed with 0.1 M PB to remove unbound AChE. The ITO/PDDA/CdS/PEDOT/AChE photoanode was obtained and stored at 4 °C when not in use.

2.4 OP assay at the photoanode

For the measurement of chlorpyrifos as the model of OPs, the obtained ITO/PDDA/CdS/PEDOT/AChE was immersed in 0.1 M PB (pH 7.4) containing different concentrations of standard chlorpyrifos and incubated for 10 min; then, it was transferred to the electrochemical cell of 5.0 mL PB (pH 7.4) containing 1 mM ATCh, an enzyme substrate, to study the photoelectrical response with visible light irradiation.

2.5 Fabrication of the CP/CNTs/AuNPs/BOD biocathode

Briefly, 8.0 mg of CNTs was dispersed in 1% PDDA salt solution containing 0.02 M NaCl (4.0 mL) and then ultrasonicated for 30 min to form a homogeneous suspension of positively charged CNTs/PDDA composites. Residual PDDA polymer was removed by centrifugation (15 000 rpm, 10 min), and the precipitate was washed with ultrapure water three times. Subsequently, the prepared CNTs/PDDA was dispersed in negatively charged AuNP solution (5 mL) and stored at 4 °C overnight. After that, excess AuNPs were removed by centrifugation (6000 rpm, 5 min), and the CNTs/AuNP precipitate was re-dissolved in ultrapure water to form a homogeneous suspension (1 mg mL^{-1}). Subsequently, 50 μL of the as-prepared suspension was casted on the surface of a carbon paper (CP, 1 × 1 cm). Then, the electrode was dried at 37 °C for 2 h, and it was further coated with 15 μL of BOD solution at 4 °C for 12 h to obtain the CP/CNTs/AuNPs/BOD biocathode.

2.6 Light-driven self-powered biosensing of OPs

A light-driven PEFC-based self-powered biosensor was constructed by using the as-prepared photoanode and biocathode at room temperature (25 °C). The supporting electrolyte was 0.1 M PB (pH 7.4) containing 1 mM ATCh. E^{OCV} of the PEFC composed of the as-prepared PDDA/CdS/PEDOT/AChE-modified photoanode and CNTs/AuNPs/BOD-modified biocathode was first measured in the supporting electrolyte; subsequently, the PDDA/CdS/PEDOT/AChE-modified photoanode was soaked in 2 mL of the target OP solution at a certain concentration and incubated for 10 min to capture the target. Then, the electrode was taken out and placed back in the electrolytic cell, and E^{OCV} of PEFC was measured again.

3. Results and discussion

3.1 Assembly and characterization of the photoanode

For the photoanode, as shown in Scheme S1 (ESI†), negatively charged CdS QDs were selected as the photoanode substrates; due to the excellent properties of strong absorption in the visible region, they could be assembled on the surface of PDDA-modified ITO electrode *via* electric interactions. Because of the high recombination rate of photogenerated carriers for CdS,[39,40] a sensitized reagent PEDOT was selected to enhance the photocurrent signal,[41] which was obtained *via* electropolymerization of EDOT at the above electrode. The formed PEDOT/CdS bi-layer heterojunction structure was in favor of the separation efficiency of hole–electron pairs because the PEDOT polymer acted as both the light absorber and the hole-transporter, whereas CdS provided the electron percolation pathway.[42] A higher photocurrent of the PEDOT/CdS photoanode could be obtained. TEM image shows that PEDOT formed from the electropolymerization of EDOT is a thin and well-distributed film (Fig. S1, ESI†). Finally, AChE was immobilized on the as-prepared PEDOT/CdS electrode surface, and the photocurrent measurement was obtained.

To verify the above assembly process, EIS was performed with $[Fe(CN)_6]^{3-/4-}$ as the redox probe, and the corresponding Nyquist plots are shown in Fig. 1A. Compared to the bare ITO with a small charge-transfer resistance (R_{ct}) value (164 Ω, curve a), the PDDA-modified ITO electrode exhibited a slightly increased R_{ct} value (173 Ω, curve b) due to poor conductivity of PDDA. Subsequently, the R_{ct} value of the CdS QD-modified electrode further increased (289 Ω, curve d) because the carboxyl group of the negatively charged CdS–COOH QDs prevented the redox probe from approaching the electrode surface. Because of the excellent conductivity of PEDOT, a decreased R_{ct} value (263 Ω, curve c) was obtained after PEDOT film modification. When AChE with high steric hindrance was continually immobilized on the electrode, the R_{ct} value gradually increased (344 Ω, curve e). The above results confirmed the successful construction of the modified photoanode.

To confirm the feasibility of the as-proposed biosensing strategy, the photocurrent response of the photoanode was first investigated, and the experiment was performed in 0.1 M PB containing 1 mM ATCh under visible light irradiation. Initially, without PEDOT film, only a relatively low photocurrent of 0.3 μA (curve a, in Fig. 1B) was obtained. In contrast, after sensitization by the PEDOT film, the photocurrent significantly increased to 0.7 μA (curve b, in Fig. 1B) due to the enhanced separation efficiency of hole–electron pairs. Moreover, in the

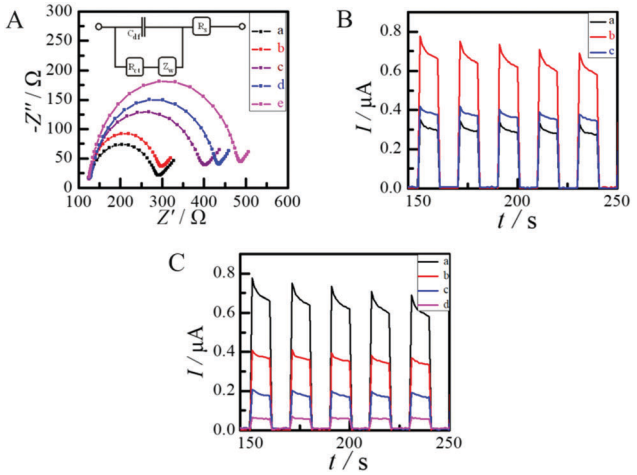

Fig. 1 (A) EIS curves of different modified ITO electrodes: (a) bare ITO electrode, (b) ITO/PDDA, (c) ITO/PDDA/CdS/PEDOT, (d) ITO/PDDA/CdS, (e) ITO/PDDA/CdS/PEDOT/AChE. (B) Photocurrent responses of (a) ITO/PDDA/CdS/AChE and ITO/PDDA/CdS/PEDOT/AChE before (b) and after (c) incubation with 0.005 μg mL^{-1} chlorpyrifos solution for 10 min. (C) Photocurrent responses of ITO/PDDA/CdS/PEDOT/AChE after incubation with (a) 0, (b) 0.002, (c) 0.01, (d) 0.1 μg mL^{-1} chlorpyrifos solutions for 10 min. The electrolyte solution was 0.1 M PB (pH 7.4) containing 1 mM ATCh.

presence of OPs, specific binding between chlorpyrifos and AChE inhibited the catalytic activity of AChE on hydrolysis reaction,[43] leading to decrease in thiocholine and thus, the photocurrent was clearly reduced to 0.4 μA (curve c, in Fig. 1B). Notably, the photocurrent gradually decreased with the increase in chlorpyrifos concentration (Fig. 1C). This target-induced signal response laid a strong foundation for the selective detection and quantification of OPs and confirmed the feasibility for biosensing based on conjugated polymer-sensitized CdS and enzyme inhibition strategy.

3.2 Optimization for the photocurrent responses at the photoanode

To achieve optimal photocurrent responses at the photoanode, CdS QD concentrations and electropolymerization times for PEDOT film were investigated. As shown in Fig. 2A, the photocurrent gradually increased with the increase in CdS QD concentration, which could be because immobilization of more CdS QDs can result in higher light utilization efficiency. Moreover, a relatively stable photocurrent signal was obtained in a wide concentration range of 1–2 μM. Thus, to obtain a sufficiently large photocurrent and to lower the expense, 2 μM CdS QDs was selected in the subsequent experiment. Furthermore, the electropolymerization time for PEDOT film is also a key factor, which determined the thickness of the PEDOT film and further influenced the photocurrent. As shown in Fig. 2B, due to insufficient electropolymerization time, the PEDOT film became very thin; in this case, a relatively low photocurrent was obtained due to inefficient sensitization. As the electropolymerization time for the PEDOT film was prolonged, the photocurrent gradually increased. However, with the increase in PEDOT thickness, the diffusion resistance of electron transfer

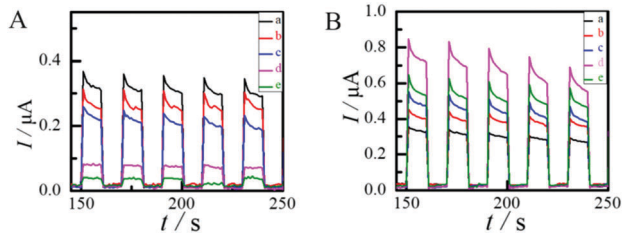

Fig. 2 (A) Photocurrent curves of the ITO/PDDA/CdS/AChE electrode under different CdS concentrations: (a) 2 μM, (b) 1.5 μM, (c) 1 μM, (d) 500 nM, (e) 200 nM in 0.1 M PB containing 1 mM ATCh. (B) Photocurrent curves with different electropolymerization times for PEDOT on the ITO/PDDA/CdS/PEDOT/AChE electrode. The electropolymerization times were (a) 400 s, (b) 500 s, (c) 600 s, (d) 700 s, (e) 800 s.

could not be ignored, which resulted in the decrease in the photocurrent response value. Thus, the time of 700 s was chosen as the optimal time of electropolymerization for the PEDOT film.

3.3 Fabrication and characterization of the biocathode

As an electron acceptor, the biocathode also played a vital role for the performance of the PEFC-based self-powered biosensor. In our study, we used CNTs/AuNPs as the substrate material for loading the cathodic enzyme BOD, which was prepared through the electrostatic interaction between positively charged CNTs and carboxyl group-functionalized AuNPs.[44] The morphology of the obtained CNTs/AuNPs was characterized by TEM. As displayed in Fig. 3A, uniform AuNPs with a size of ~10 nm were homogeneously decorated on the surface of two-dimensional CNTs, which indicated the successful fabrication of CNTs/AuNPs. Subsequently, the enzyme BOD was immobilized on the CNTs/AuNP electrode through a condensation reaction between the amino groups in the enzyme structure and the carboxyl groups on AuNPs on the above electrode. To confirm the biocatalysis performance of the biocathode, CVs were measured under different conditions. As shown in Fig. S2 (ESI†), CV curves was almost no change in the presence or absence of O_2, implying the substrate materials CNTs/AuNPs have no catalytic ability for O_2. However, when the CNTs/AuNP electrode was modified by the enzyme BOD, a clear reduction current was observed in the presence of O_2 compared to that under N_2 (Fig. 3B), which suggested that the CNTs/AuNPs/BOD biocathode exhibited excellent electrocatalytic activity for oxygen reduction. The obtained results from the photoanode and

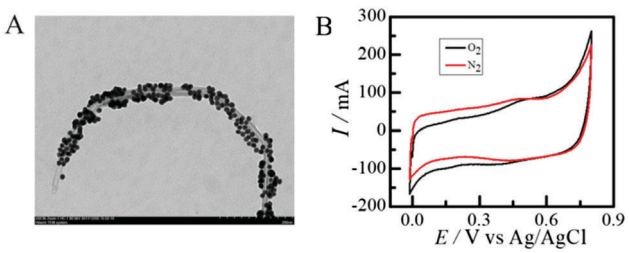

Fig. 3 (A) TEM image of CNTs/AuNPs. (B) CVs of the CNTs/AuNP BOD biocathode in PB (pH = 7.4) saturated with N_2 or O_2. Scan rate = 50 mV s^{-1}.

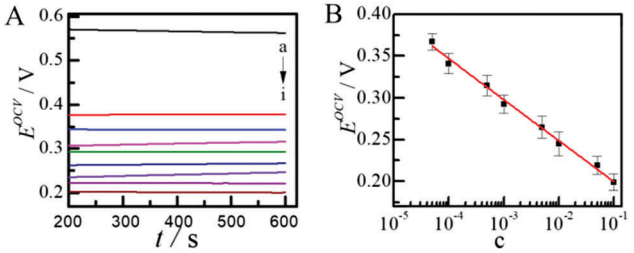

Fig. 4 (A) E^{OCV} of the proposed sensors with different concentrations of OPs in 0.1 M PB (pH 7.4) containing 1 mM ATCh: (a–i) 0, 0.00005, 0.0001, 0.0005, 0.001, 0.005, 0.01, 0.05, 0.1 μg mL^{-1}. (B) The plot of E^{OCV} *vs.* the logarithm of OP concentration. Error bars represent the standard deviation of an average value from independent measurements of three biosensors.

biocathode laid a strong foundation for the assembly of the light-driven self-powered biosensor.

3.4 PEFC-based self-powered biosensing platform for OP analysis

By combining the ITO/CdS/PEDOT/AChE photoanode and the CP/CNTs/AuNPs/BOD biocathode, a PEFC-based self-powered biosensor was constructed to realize chlorpyrifos detection. The performance of the as-proposed biosensor was evaluated with different concentrations of chlorpyrifos under optimal experimental conditions. As shown in Fig. 4A, in the absence of OPs, E^{OCV} of the biosensor was about 0.57 V (curve a). As OPs were added, there was a negative correlation between E^{OCV} and OP concentration (curves b–i). Furthermore, a linear relationship was well-fitted between E^{OCV} and the logarithm of OP concentration in the range from 0.00005 to 0.1 μg mL^{-1} (Fig. 4B). The linear equation was $E^{OCV} = 0.15 - 0.049 \log c$, and the coefficient of determination (R^2) was 0.9943. The detection limit was calculated to be 0.012 ng mL^{-1} (S/N = 3). In addition, the as-prepared PEFC-based self-powered biosensing platform showed a wider linear range and a comparable or lower detection limit for OP detection than previously reported AChE-based biosensors, as shown in Table S1 (ESI†).

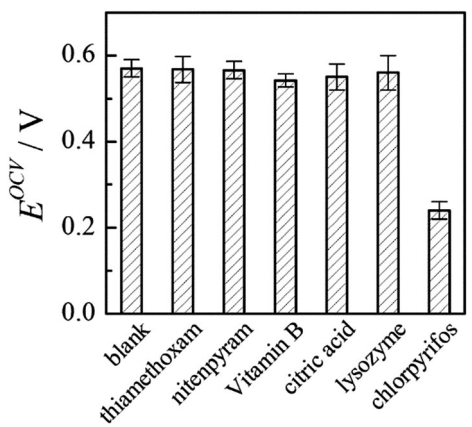

Fig. 5 Selectivity analysis for chlorpyrifos detection by monitoring E^{OCV} with 0.01 μg mL^{-1} of interferences (thiamethoxam, nitenpyram, vitamin B, citric acid, and lysozyme) and 0.01 μg mL^{-1} chlorpyrifos.

3.5 Selectivity of the PEFC-based self-powered biosensor

Selectivity is also a key factor for evaluating the property of a biosensor. To investigate the selectivity, two pesticides (thiamethoxam and nitenpyram), vitamin (vitamin B), organic acid (citric acid), and enzymes (lysozyme) were used as interferences. As shown in Fig. 5, only chlorpyrifos could inhibit the catalytic activity of AChE, indicating the high selectivity of the as-proposed biosensor for OPs over other interferences. The results demonstrated that the as-proposed biosensor has great potential in practical applications.

4. Conclusions

In summary, we proposed, for the first time, a new photoelectrochemical self-powered biosensing platform for ultrasensitive OP assay *via* integration of the co-sensitized PEDOT/CdS photoanode and enzyme inhibition strategy. As no external power source and anodic enzyme were needed, the as-designed self-powered sensing platform exhibited unique advantages of simple instrumentation, portability and low cost. In addition, because of the co-sensitized PEDOT/CdS photoanode and enzyme inhibition strategy, the enhanced separation efficiency of hole-electron pairs endowed the biosensor with high sensitivity for sensing OPs, which was comparable or superior to those of other biosensors reported previously. The proposed strategy not only offers a new perspective for the development of PEFC-based self-powered sensors, but is also expected to become a general consideration for constructing sensing platforms for environmental pollutants and food safety.

Conflicts of interest

There are no conflicts of interest to declare.

Acknowledgements

We gratefully appreciate the financial support from the National Natural Science Foundation of China (21605092, 21775082 and 21575074), the Natural Science Foundation of Shandong Province, China (ZR2016BQ08), Major Program of Shandong Province Natural Science Foundation (ZR2018ZC0127), the Research Foundation for Distinguished Scholars of Qingdao Agricultural University (663-1117002), and the Special Foundation for Taishan Scholar of Shandong Province (No. ts201511052).

Notes and references

1 M. Zhou, *Electroanalysis*, 2015, **27**, 1786–1810.
2 E. Katz, A. F. B. And and I. Willner, *J. Am. Chem. Soc.*, 2001, **123**, 10752–10753.
3 B. Cakiroglu and M. Ozacar, *Biosens. Bioelectron.*, 2018, **119**, 34–41.
4 K. Yan, Y. Zhu, W. Ji, F. Chen and J. Zhang, *Anal. Chem.*, 2018, **90**, 9662–9666.

5 L. Fu, J. Liu, Z. Hu and M. Zhou, *Electroanalysis*, 2018, DOI: 10.1002/elan.201800487.
6 P. P. Gai, Y. S. Ji, W. J. Wang, R. B. Song, C. Zhu, Y. Chen, J. R. Zhang and J. J. Zhu, *Nano Energy*, 2016, **19**, 541–549.
7 F. Wu, P. Yu and L. Mao, *Chem. Soc. Rev.*, 2017, **46**, 2692–2704.
8 P. P. Gai, C. C. Gu, T. Hou and F. Li, *ACS Appl. Mater. Interfaces*, 2018, **10**, 9325–9331.
9 J. Ouyang, Z. Liu, Y. Han, K. Zeng, J. Sheng, L. Deng and Y. N. Liu, *ACS Appl. Mater. Interfaces*, 2016, **8**, 35004–35011.
10 G. K. C. dos Santos, F. G. S. da Silva, S. Yotsumoto Neto, W. T. P. dos Santos, R. de Cássia Silva Luz and F. S. Damos, *Electroanalysis*, 2018, **30**, 1742–1748.
11 D. Wen, L. Deng, S. Guo and S. Dong, *Anal. Chem.*, 2011, **83**, 3968–3972.
12 W. Liu, Z. Zhou, L. Yin, Y. Zhu, J. Zhao, B. Zhu, L. Zheng, Q. Jin and L. Wang, *Sens. Actuators, B*, 2018, **271**, 247–255.
13 K. Yan, Y. Yang and J. Zhang, *Sens. Actuators, B*, 2018, **259**, 394–401.
14 H. He, C. Dong, Y. Fu, W. Han, T. Zhao, L. Xing and X. Xue, *Sens. Actuators, B*, 2018, **267**, 392–402.
15 R. Saraf and V. Maheshwari, *ACS Appl. Mater. Interfaces*, 2018, **10**, 21066–21072.
16 D. Majdecka, S. Draminska, D. Janusek, P. Krysinski and R. Bilewicz, *Biosens. Bioelectron.*, 2018, **102**, 383–388.
17 C. E. Zhao, P. P. Gai, R. B. Song, Y. Chen, J. R. Zhang and J. J. Zhu, *Chem. Soc. Rev.*, 2017, **46**, 1545–1564.
18 L. Zhang, M. Zhou and S. Dong, *Anal. Chem.*, 2012, **84**, 10345–10349.
19 P. N. Bartlett and F. A. Al-Lolage, *J. Electroanal. Chem.*, 2018, **819**, 26–37.
20 R. D. Milton and S. D. Minteer, *J. R. Soc., Interface*, 2017, **14**, 20170253.
21 J. Tian, H. Zhu, J. Chen, X. Zheng, H. Duan, K. Pu and P. Chen, *Small*, 2017, **13**, 1700798.
22 L. Han, S. Guo, P. Wang and S. Dong, *Adv. Energy Mater.*, 2015, **5**, 1400424.
23 L. Han, L. Bai, C. Zhu, Y. Wang and S. Dong, *Chem. Commun.*, 2012, **48**, 6103–6105.
24 C. Gao, L. Zhang, Y. Wang, J. Yu and X. Song, *Biosens. Bioelectron.*, 2016, **83**, 327–333.
25 W. X. Dai, L. Zhang, W. W. Zhao, X. D. Yu, J. J. Xu and H. Y. Chen, *Anal. Chem.*, 2017, **89**, 8070–8078.
26 B. Peng, L. Tang, G. Zeng, S. Fang, X. Ouyang, B. Long, Y. Zhou, Y. Deng, Y. Liu and J. Wang, *Biosens. Bioelectron.*, 2018, **121**, 19–26.
27 Y. Zhang, Y. Li, W. Sun, C. Yuan, B. Wang, W. Zhang and X. M. Song, *Langmuir*, 2017, **33**, 12065–12071.
28 H. Yang, Z. H. Wang, Y. Y. Zheng, L. Q. He, C. Zhan, X. Lu, Z. Q. Tian, P. P. Fang and Y. Tong, *J. Am. Chem. Soc.*, 2016, **138**, 16204–16207.
29 J. W. Zhou, X. M. Zou, S. H. Song and G. H. Chen, *J. Agric. Food Chem.*, 2018, **66**, 1307–1319.
30 A. Sahin, K. Dooley, D. M. Cropek, A. C. West and S. Banta, *Sens. Actuators, B*, 2011, **158**, 353–360.
31 H. Dzudzevic Cancar, S. Soylemez, Y. Akpinar, M. Kesik, S. Goker, G. Gunbas, M. Volkan and L. Toppare, *ACS Appl. Mater. Interfaces*, 2016, **8**, 8058–8067.
32 H. F. Cui, W. W. Wu, M. M. Li, X. Song, Y. Lv and T. T. Zhang, *Biosens. Bioelectron.*, 2018, **99**, 223–229.
33 X. Z. Wang, S. S. Dong, T. Hou, L. Liu, X. J. Liu and F. Li, *Analyst*, 2016, **141**, 1830–1836.
34 R. Bala, M. Kumar, K. Bansal, R. K. Sharma and N. Wangoo, *Biosens. Bioelectron.*, 2016, **85**, 445–449.
35 H. Li, J. Li, Q. Xu and X. Hu, *Anal. Chem.*, 2011, **83**, 9681–9686.
36 K. Vikrant, D. C. W. Tsang, N. Raza, B. S. Giri, D. Kukkar and K. H. Kim, *ACS Appl. Mater. Interfaces*, 2018, **10**, 8797–8817.
37 J. F. Chang, H. Y. Li, T. Hou and F. Li, *Biosens. Bioelectron.*, 2016, **86**, 971–977.
38 Y. Wang, L. Ge, P. Wang, M. Yan, J. Yu and S. Ge, *Chem. Commun.*, 2014, **50**, 1947–1949.
39 O. K. Okoth, K. Yan, J. Feng and J. Zhang, *Sens. Actuators, B*, 2018, **256**, 334–341.
40 I. Ibrahim, H. N. Lim, R. Mohd Zawawi, A. Ahmad Tajudin, Y. H. Ng, H. Guo and N. M. Huang, *J. Mater. Chem. B*, 2018, **6**, 4551–4568.
41 G. Wang, A. Morrin, M. Li, N. Liu and X. Luo, *J. Mater. Chem. B*, 2018, **6**, 4173–4190.
42 G. F. Samu, C. Visy, K. Rajeshwar, S. Sarker, V. R. Subramanian and C. Janáky, *Electrochim. Acta*, 2015, **151**, 467–476.
43 W. Zhao, P. Y. Ge, J. J. Xu and H. Y. Chen, *Environ. Sci. Technol.*, 2009, **43**, 6724–6729.
44 M. Zhao, Y. Gao, J. Sun and F. Gao, *Anal. Chem.*, 2015, **87**, 2615–2622.